FREE CONVECTION HEAT LOSSES IN A FLAT PLATE SOLAR COLLECTOR

Kristian Lenić, Bernard Franković
Faculty of Engineering University of Rijeka, Vukovarska 58, HR-51000 Rijeka, Croatia
Phones: + 385 51 651 518, 651 506, Fax: + 385 51 675 801,
E-mails: lenick@riteh.hr, bernardf@riteh.hr

Abstract: *In the paper the free convection heat looses inside closed air container with isothermal non-uniform boundary condition has been analysed numerically. The mathematical model based on Oberbeck mathematical model of boundary layer has been defined. This model has been used to solve the two-dimensional transient heat transfer problem. Fields of relevant thermodynamic dimensions' characteristics, such as velocity vectors, stream function and temperature gradient have been calculated using finite volume numerical method. A computer solver for transient two-dimensional heat transfer has been developed. The influence of Rayleigh number on different flow and heat convection regimes has been analysed for different inclination angles. An impact of different flow regimes on heat convection has been also analysed using local and average Nusselt numbers. Results have been applied to prediction of free convection heat losses in an approximated model of solar collector for different inclination angles.*

Key words: free convection heat looses, solar collector, finite volume method, heat losses, Rayleigh number, local and average Nusselt number

1. INTRODUCTION

Many research activities in a field of free convection inside of an enclosed container deal with so-called Rayleigh-Benard problem due to its wide application in engineering practice. Characteristic boundary conditions for this kind of free-convection problem are: the bottom surface of the container is held at relatively high temperature ("hot surface"), the top surface is held at relatively low temperature ("cold surface") while the side walls are adiabatic (figure 1). Under this conditions the flow undergoes through different types of regimes depending on Rayleigh number. Pure conduction is a primary state, then, by increasing of *Ra* number, the flow changes from steady cellular flows, transient periodical flows, quasi-periodical flows to unpredictable transient flows. This phenomena appears due to instability of flow under described boundary conditions. The situation becomes more complex when some inclination angles or different aspect ratio are applied to the domain. Many authors have examined flow and heat transfer under these various types of boundary conditions. In this research, the "hot surface" is substituted with linear distribution of temperature on the wall. Other boundary conditions are like these used to simulate Rayleigh-Benard problem. Applied boundary conditions are shown on figure 2.

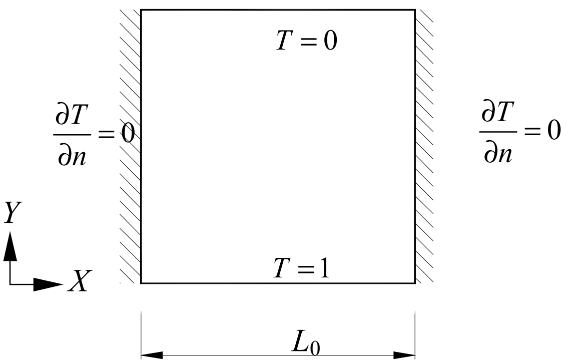

Figure 1. Typical boundary conditions of Rayleigh-Benard free convection problem

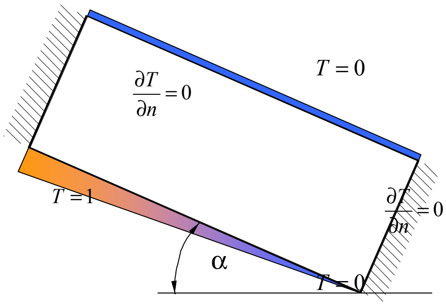

Figure 2. Domain with boundary condition of linear temperature distribution applied on one boundary

2. NUMERICAL AND MATHEMATICAL MODELS

Mathematical model is defined using equations of conservation for two-dimensional transient fluid flow and heat transfer. The analysed container is fulfilled with air, Pr=0,73. Air has been considered as viscous, non-compressible Newtonian fluid. In the analysed case fluid flow and heat transfer are driven by buoyancy effect so the additional equation must be used. Concerning these conditions, a Boussinesq approximation that describes linear relation between density and temperature, has also been added to complete mathematical model. So, fluid density has been considered constant in all circumstances except for description of gravity forces in momentum equations where the mentioned approximation has been used. Considering constant density and two-dimensional fluid flow the continuity equation may be written as:

$$\frac{\partial u_x}{\partial x}+\frac{\partial u_y}{\partial y}=0 \tag{1}$$

Using (1) the momentum equations are:

$$x\ \ldots \qquad \rho\left(\frac{\partial u_x}{\partial t}+u_x\frac{\partial u_x}{\partial x}+u_y\frac{\partial u_x}{\partial y}\right)=\rho g_x-\frac{\partial p}{\partial x}+\eta\left(\frac{\partial^2 u_x}{\partial x^2}+\frac{\partial^2 u_x}{\partial y^2}\right) \tag{2}$$

$$y \ldots \qquad \rho\left(\frac{\partial u_y}{\partial t} + u_x \frac{\partial u_y}{\partial x} + u_y \frac{\partial u_y}{\partial y}\right) = \rho g_y - \frac{\partial p}{\partial y} + \eta\left(\frac{\partial^2 u_y}{\partial x^2} + \frac{\partial^2 u_y}{\partial y^2}\right) \tag{3}$$

Energy equation can be written as:

$$\frac{\partial T}{\partial t} + u_x \frac{\partial T}{\partial x} + u_y \frac{\partial T}{\partial y} = a\left(\frac{\partial^2 T}{\partial x^2} + \frac{\partial^2 T}{\partial y^2}\right) + \frac{q_i}{\rho c} \tag{4}$$

Boussinesq approximation is defined as follows:

$$\rho = \rho_0\left[1 - \beta(T - T_0)\right] \tag{5}$$

where ρ is density and T temperature of fluid. ρ_0 denotes density of fluid at the temperature T_0 and β is the thermal expansion coefficient.

Using (5) equations (2) and (3) become:

$$x \ldots \qquad \frac{\partial u_x}{\partial t} + u_x \frac{\partial u_x}{\partial x} + u_y \frac{\partial u_x}{\partial y} = -\frac{1}{\rho}\frac{\partial p^*}{\partial x} - \beta(T - T_0)g_x + \nu\left(\frac{\partial^2 u_x}{\partial x^2} + \frac{\partial^2 u_x}{\partial y^2}\right) \tag{6}$$

$$y \ldots \qquad \frac{\partial u_y}{\partial t} + u_x \frac{\partial u_y}{\partial x} + u_y \frac{\partial u_y}{\partial y} = -\frac{1}{\rho}\frac{\partial p^*}{\partial y} - \beta(T - T_0)g_y + \nu\left(\frac{\partial^2 u_y}{\partial x^2} + \frac{\partial^2 u_y}{\partial y^2}\right) \tag{7}$$

where p^* denotes pressure value not including gravity influence (hydrostatic component):

$$p^* = p - \rho_0 g h \tag{8}$$

Equations of conservation have been translated in dimensionless form in order to simplify the calculation, comparison and application of numerical results. Several dimensionless variables have been defined as follows:

- dimensionless coordinates:

$$X = \frac{x}{L_0} \;\Rightarrow\; x = L_0 \cdot X \tag{9}$$

$$Y = \frac{y}{L_0} \;\Rightarrow\; y = L_0 \cdot Y \tag{10}$$

- dimensionless velocity components:

$$W_x = \frac{u_x}{W_0} \;\Rightarrow\; u_x = W_0 \cdot W_x \tag{11}$$

$$W_y = \frac{u_y}{W_0} \;\Rightarrow\; u_y = W_0 \cdot W_y \tag{12}$$

- dimensionless time:

$$\tau = \frac{t}{\frac{L_0}{W_0}} \;\Rightarrow\; t = \tau \cdot \frac{L_0}{W_0} \tag{13}$$

- dimensionless pressure:

$$P = \frac{p^*}{\rho \cdot W_0^2} \;\Rightarrow\; p^* = \rho W_0^2 P \tag{14}$$

- and dimensionless temperature:

$$\vartheta = \frac{T - T_0}{T_1 - T_0} = \frac{T - T_0}{\Delta T} \quad \Rightarrow \quad T = T_0 + \frac{\vartheta}{\Delta T}. \tag{15}$$

Rayleigh and Prandtl numbers are defined as:

$$Ra = \frac{g\beta \Delta T L_0^{\,3}}{a \cdot \nu}, \tag{16}$$

$$Pr = \frac{\nu}{a} \tag{17}$$

Concerning (9)-(17), momentum equations in dimensionless form become:

$$x \ldots \quad \frac{\partial W_x}{\partial \tau} + W_x \frac{\partial W_x}{\partial X} + W_y \frac{\partial W_x}{\partial Y} = -\frac{\partial P}{\partial X} - \frac{g_x}{g}\vartheta + \sqrt{\frac{Pr}{Ra}} \left(\frac{\partial^2 W_x}{\partial X^2} + \frac{\partial^2 W_x}{\partial Y^2} \right) \tag{18}$$

$$y \ldots \quad \frac{\partial W_y}{\partial \tau} + W_x \frac{\partial W_y}{\partial X} + W_y \frac{\partial W_y}{\partial Y} = -\frac{\partial P}{\partial Y} - \frac{g_y}{g}\vartheta + \sqrt{\frac{Pr}{Ra}} \left(\frac{\partial^2 W_y}{\partial X^2} + \frac{\partial^2 W_y}{\partial Y^2} \right) \tag{19}$$

Energy equation in dimensionless form is:

$$\frac{\partial \vartheta}{\partial \tau} + W_x \frac{\partial \vartheta}{\partial X} + W_y \frac{\partial \vartheta}{\partial Y} = \frac{1}{\sqrt{Ra \cdot Pr}} \left(\frac{\partial^2 \vartheta}{\partial X^2} + \frac{\partial^2 \vartheta}{\partial Y^2} \right) \tag{20}$$

Only two types of boundary conditions have been used. Adiabatic boundary condition has been applied on two opposite walls and can be defined with following settings: $u_x = 0$, $u_y = 0$ and $\frac{\partial T}{\partial x} = 0$ or $\frac{\partial T}{\partial y} = 0$ depending on wall orientation.

Geometrical boundary condition is applied to walls with pre-set temperature value. The pre-set wall temperature can be constant or linearly distributed along the wall length. Settings, which describe this boundary condition, are: $u_x = 0$, $u_y = 0$ and $T = T_{preset}(x)$ or $T = T_{preset}(y)$ depending on wall orientation.

Heat transfer intensity can be analysed by average and local values of Nusselt number. Local Nusselt number is defined as:

$$Nu = \left(\frac{\partial T}{\partial n} \right)_S. \tag{21}$$

Average intensity of heat transfer through boundary can be described with average Nusselt number, which is defined as:

$$\overline{Nu} = \frac{\iint_S Nu \, \mathrm{d}S}{\iint_S \mathrm{d}S}. \tag{22}$$

This mathematical model has been solved numerically using finite volume method. To interpolate values of dependent variables between grid nodes a power-law scheme has been assumed. For the numerical calculation a computer solver for transient two-dimensional heat and fluid flow has been developed. The algorithm of computer software bases on revised Semi-Implicit Method of Pressure-Linked Equations (revised SIMPLE = SIMPLER). Calculation of temperature and velocity fields as well as local Nusselt numbers on "hot" wall has been carried out for domain aspect ratio 1:20 and for inclination angles of 0, 30, 45, 60 and 90°. For the numerical calculation the structured rectangular grid with 10x200 finite volumes has been generated and solved for different Rayleigh numbers, $Ra = 10^5$, 10^6, $2{,}5\cdot10^6$ and $5\cdot10^6$.

3. RESULTS OF NUMERICAL ANALYSIS

Applying boundary conditions presented on figure 2 as results of numerical simulations the velocity vectors, streamlines and isotherms have been obtained as well as local and average Nusselt numbers on a heated boundary.

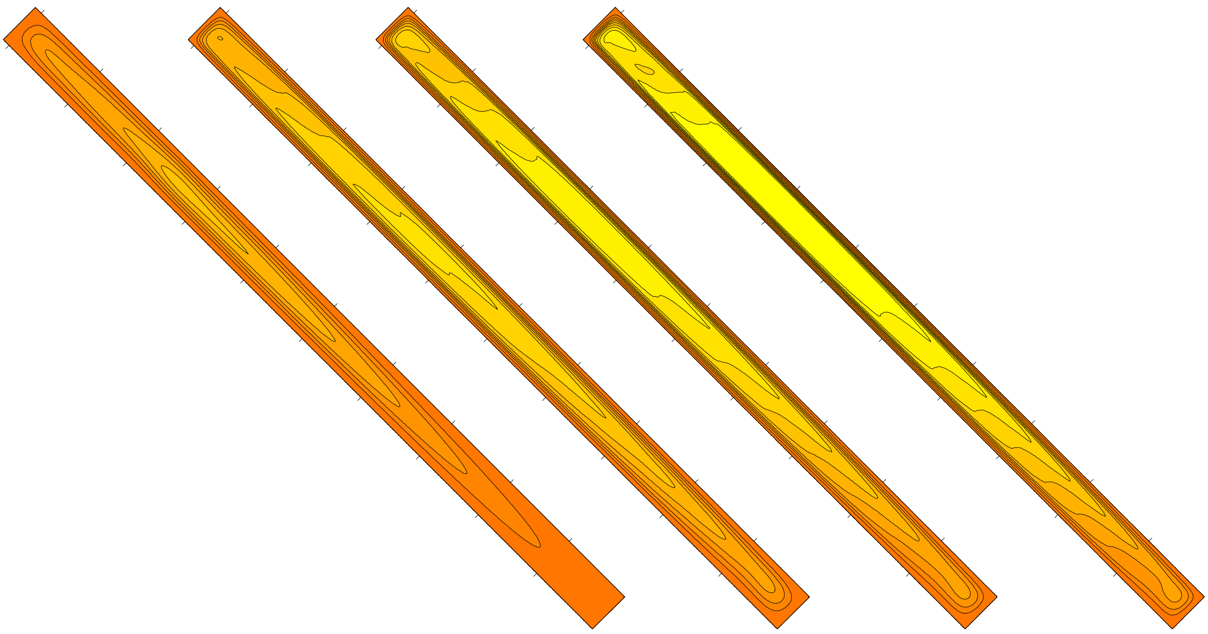

Figure 3. Streamlines for $Ra = 10^5$, 10^6, $2{,}5\cdot10^6$ and $5\cdot10^6$ – inclination angle 45°.

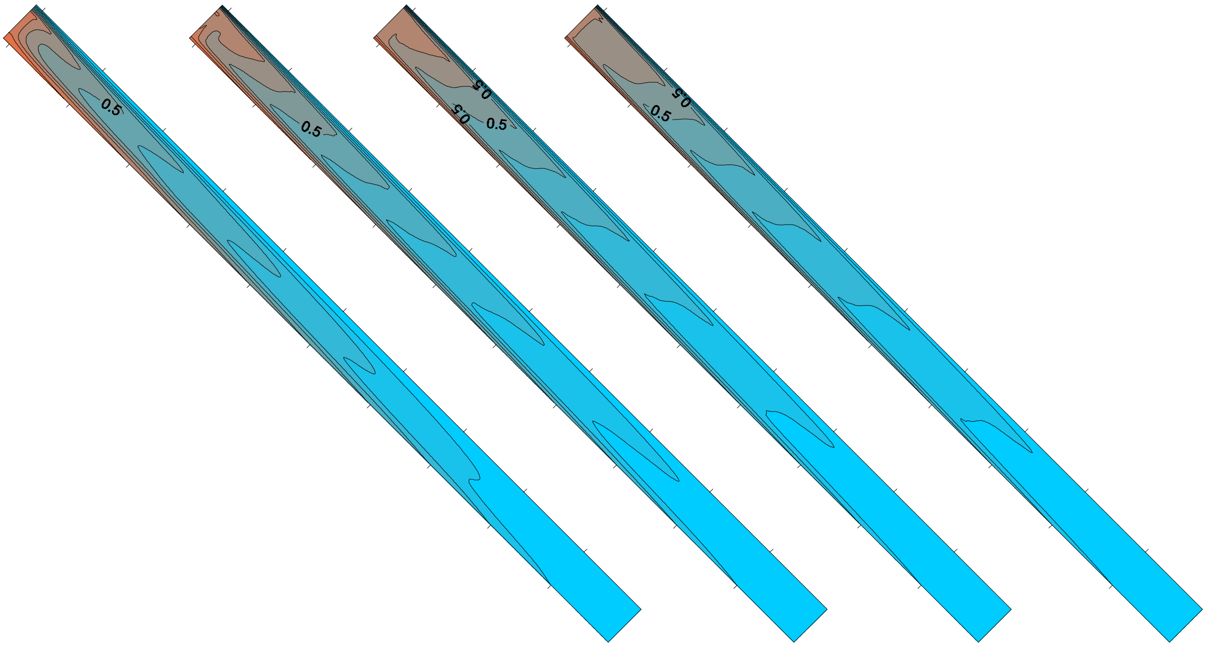

Figure 4. Isotherms for $Ra = 10^5$, 10^6, $2{,}5 \cdot 10^6$ and $5 \cdot 10^6$ – inclination angle 45°

The numerical calculation has been carried out for all mentioned ranges of inclination angles and Rayleigh numbers. The streamlines and the isotherms have been shown only for inclination angle of 45°. Streamlinnes and isotherms for $Ra = 10^5$, 10^6, $2{,}5 \cdot 10^6$ and $5 \cdot 10^6$ and for inclination angle of 45° are shown on figures 3 and 4 respectively. Local Nusselt numbers on a heated wall for different regimes and inclination angles are sown on figures 5-8.

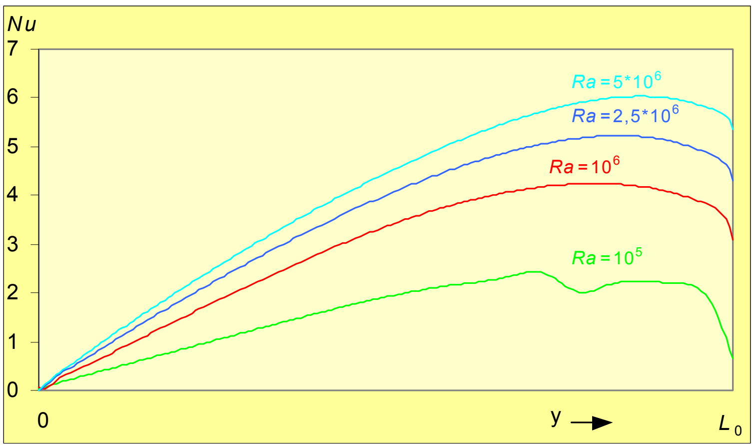

Figure 5. Local Nusselt numbers on a heated boundary for different regimes of free convection (different Ra numbers), aspect ratio $a/b = 20$ and inclination angle $\alpha = 45°$

Minimal and maximal local and average Nusselt numbers on a heated boundary for different inclination angles and for different regimes of free convection (different Ra numbers) are presented in tables 1-4.

Table 1. Minimal and maximal local and average Nusselt numbers on a heated boundary for 45° inclination angle and for different regimes of free convection (different Ra numbers).

	$Ra = 10^5$	$Ra = 10^6$	$Ra = 2{,}5 \cdot 10^6$	$Ra = 5 \cdot 10^6$
Nu_{max}	2,61	2,63	4,83	17,00
Nu_{min}	0,04	0,05	0,01	0,09
$\overline{Nu}$	0,86	1,53	2,87	9,03

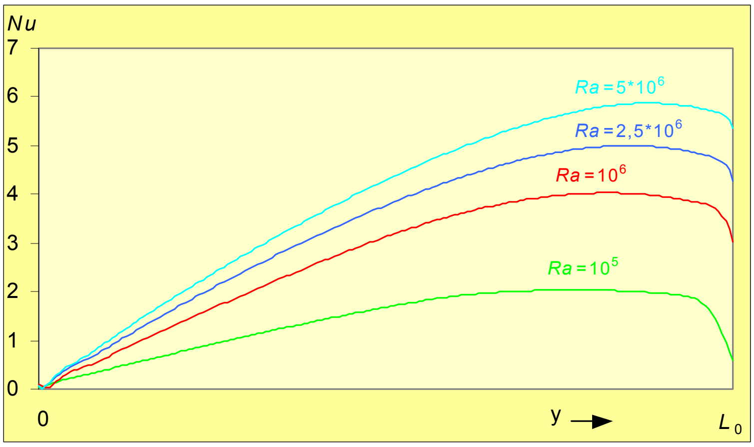

Figure 6. Local Nusselt numbers on a heated boundary for different regimes of free convection (different Ra numbers), aspect ratio *a/b* = 20 and inclination angle $\alpha = 30°$

Table 2. Minimal and maximal local and average Nusselt numbers on a heated boundary for 30° inclination angle and for different regimes of free convection (different Ra numbers).

	$Ra = 10^5$	$Ra = 10^6$	$Ra = 2{,}5 \cdot 10^6$	$Ra = 5 \cdot 10^6$
Nu_{max}	2,04	4,03	5,00	5,87
Nu_{min}	0,02	0,03	0,01	0,01
$\overline{Nu}$	1,39	2,69	3,32	3,84

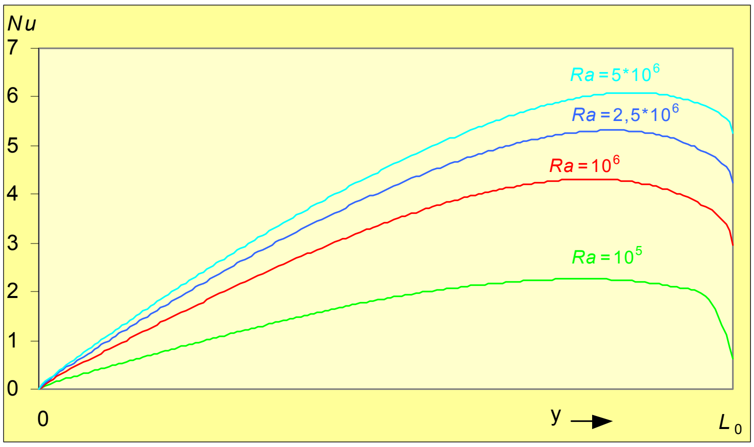

Figure 7. Local Nusselt numbers on a heated boundary for different regimes of free convection (different Ra numbers), aspect ratio *a/b* = 20 and inclination angle α = 60°

Table 3. Minimal and maximal local and average Nusselt numbers on a heated boundary for 60° inclination angle and for different regimes of free convection (different Ra numbers).

	$Ra = 10^5$	$Ra = 10^6$	$Ra = 2{,}5 \cdot 10^6$	$Ra = 5 \cdot 10^6$
Nu_{max}	2,26	4,31	5,32	6,09
Nu_{min}	0,02	0,01	0,01	0,02
$\overline{Nu}$	1,54	2,91	3,57	4,03

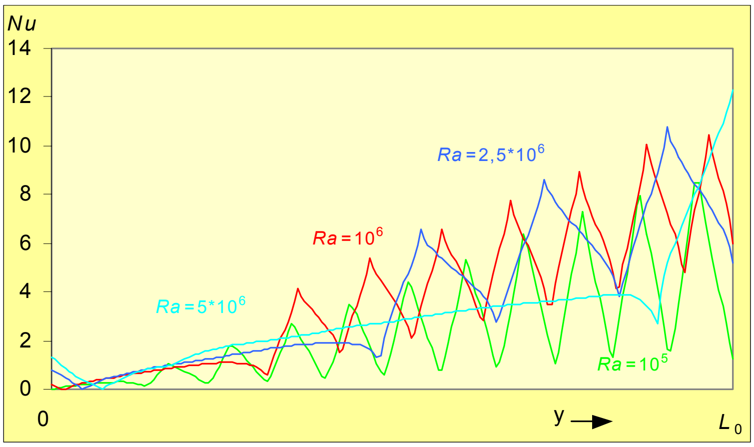

Figure 8. Local Nusselt numbers on a heated boundary for different regimes of free convection (different Ra numbers), aspect ratio *a/b* = 20 and inclination angle α = 0° (horizontal position)

Table 4. Minimal and maximal local and average Nusselt numbers on a heated boundary for 0° inclination angle and for different regimes of free convection (different Ra numbers).

	$Ra = 10^5$	$Ra = 10^6$	$Ra = 2{,}5 \cdot 10^6$	$Ra = 5 \cdot 10^6$
Nu_{max}	8,48	10,42	10,76	12,32
Nu_{min}	0,02	0,03	0,01	0,03
$\overline{Nu}$	2,41	3,78	3,71	3,02

Ranges of Nusselt numbers depending on inclination angle for different Rayleigh numbers are shown on figures 9 and 10. The dependence of average Nusselt numbers as well as maximal and minimal local Nusselt numbers on inclination angles can be seen from figures 11-14.

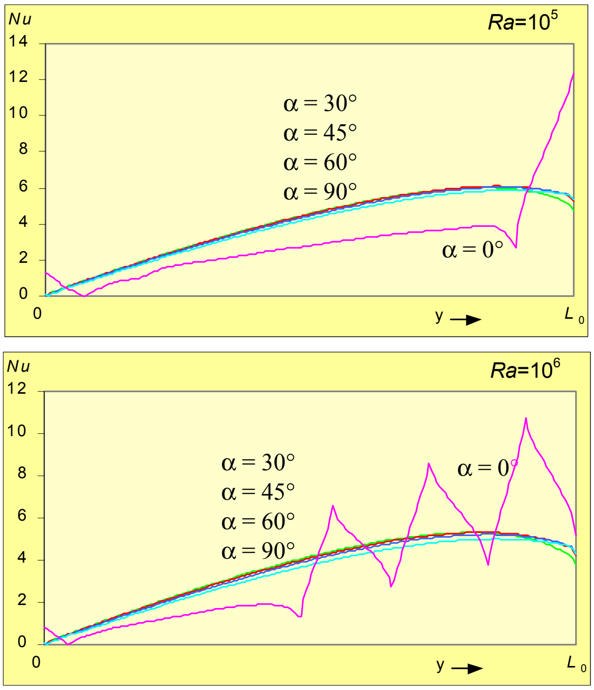

Figure 9. Local Nusselt numbers along non-uniform isothermal boundary for $Ra=10^5$ and $Ra=10^6$

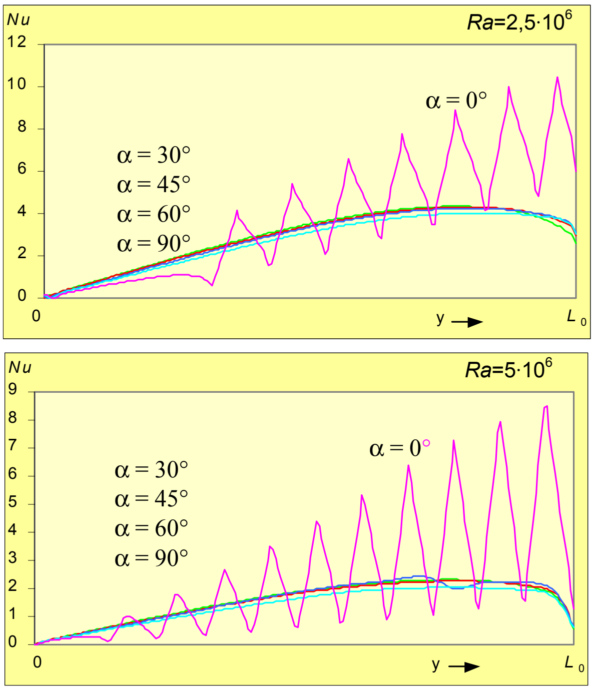

Figure 10. Local Nusselt numbers along non-uniform isothermal boundary for Ra=2,5·10^6 and Ra=5·10^6

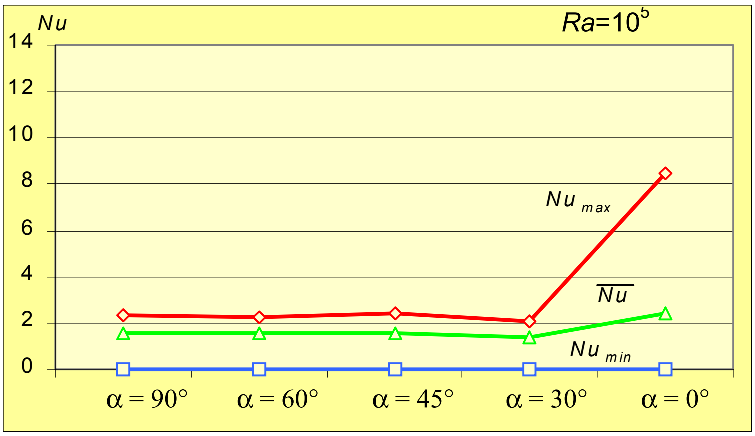

Figure 11. Dependency of minimal and maximal local and average Nusselt numbers on different inclination angles for Ra=10^5

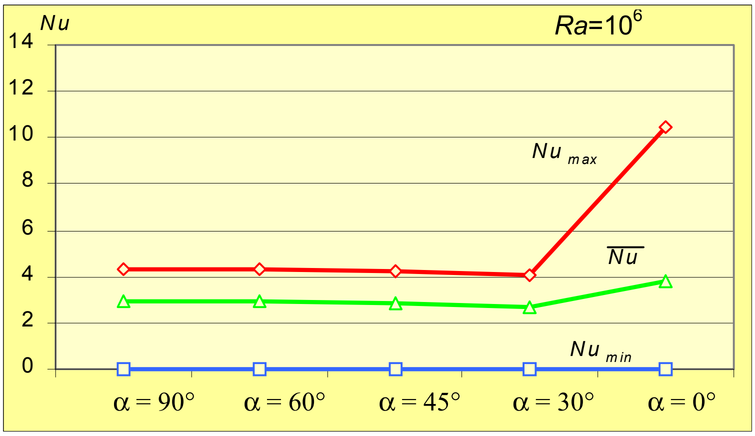

Figure 12. Dependency of minimal and maximal local and average Nusselt numbers on different inclination angles for $Ra=10^6$

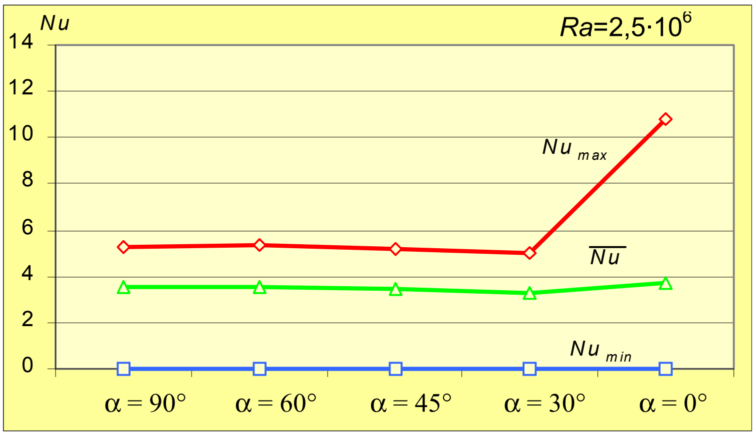

Figure 13. Dependency of minimal and maximal local and average Nusselt numbers on different inclination angles for $Ra=2{,}5\cdot10^6$

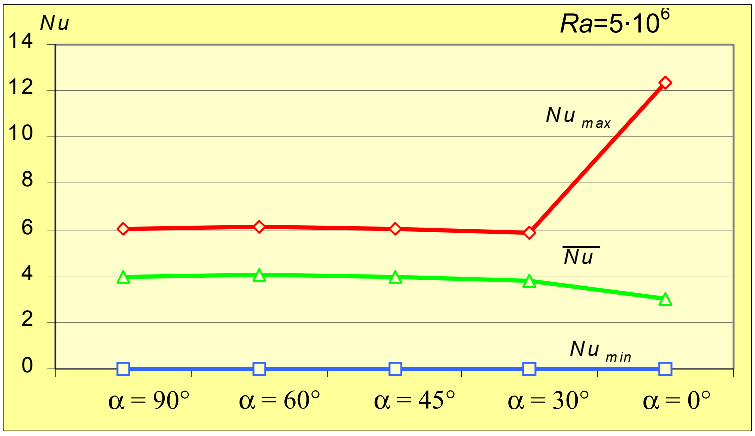

Figure 14. Dependency of minimal and maximal local and average Nusselt numbers on different inclination angles for $Ra=5\cdot10^6$

4. CONCLUSION

From the presented results can be noted that the intensity of heat transfer grows as Rayleigh number grows even if on one wall the non-uniform isothermal boundary condition is applied. For small inclination angles (α<30°), when the position is almost horizontal, a distribution of local Rayleigh numbers is notable non-uniform, since some closed flow cycles appear. In that case the number of closed cycles grows as Rayleigh number raises. Although the average Nusselt number is high, heat transfer is locally more non-uniformly distributed for $Ra=5\cdot10^6$ than for $Ra=10^5$. For these small inclination angles, the difference of maximal and minimal local Nusselt number is higher. Overall heat transfer from heated wall to the air is enhanced since closed flow cycles shift thermal energy to the centre of domain.
When the higher inclination angles are used (α>30°), further angle increasing do not affect significantly the distribution and intensity of heat transfer, regardless of Rayleigh number value. In this case it can be concluded that the distribution and intensity of local Nusselt numbers mainly depend on Rayleigh number regardless of inclination angle. Local Nusselt numbers at $Ra= 2,5\cdot10^6$ are two times higher than for $Ra=10^5$.
Regarding the fact that local and average Nusselt numbers do not significantly depend on inclination angles higher then 30° it can be concluded that is not possible to reduce convective heat losses by changing the inclination of conventional solar collector.

5. LIST OF SYMBOLS

a	thermal diffusivity (m^2/s)
c	specific heat (J/kg k)
h	height (m)
g	acceleration of gravity (m/s^2)
g_x, g_y	components of g in x and y dimension (m/s^2)
L_0	referent length (m)
Nu	Nusselt number
$\vec{n}$	vector perpendicular on boundary surface of control volume
P	dimensionless pressure
p	pressure (Pa)
Pr	Prandtl number
q_i	specific internal heat source (J/m^3)
Ra	Rayleigh number
S	surface (m^2)
t	time (s)
T	temperature (K)
T_0	minimal temperature (K)
T_1	maximal temperature (K)
ΔT	difference of maximal and minimal temperature $\Delta T = T_1 - T_0$ (K)
u_x	velocity component in x direction (m/s)
u_y	velocity component in y direction (m/s)
W_x	dimensionless velocity component in x direction
W_y	dimensionless velocity component in y direction
W_0	referent velocity (m/s)

X, Y dimensionless coordinates
x,y coordinates (m)

β thermal expansion coefficient (K^{-1})
η dynamic viscosity (Pa s)
ϑ dimensionless temperature
ν kinematic viscosity (m^2/s)
ρ density (kg/m^3)
τ dimensionless time

6. REFERENCES

[1] H. K. Versteeg, W. Malalasekera, An introduction to computational fluid dynamics – The finite volume method, Longman Scientific & Technical, Essex, 1995.
[2] J. H. Ferziger, M. Perić, Computational Methods for Fluid Dynamics, Springer, Verlag, 1996.
[3] J. H. Curry, J. R. Herring, J. Lončarić, S. A. Orszag, Order and disorder in two- and three-dimensional Benard convection, Journal of Fluid Mechanics, 1984, vol. 147, 1-38.
[4] J. N. Kostner, U. Muller, Free convection in vertical gaps, Journal of Fluid Mechanics, 1982, vol. 125, 429-451.
[5] D.R. Chenoweth, S. Paolucci, Natural convection in an enclosed vertical air layer with large horizontal temperature differences, Journal of Fluid Mechanics, 1986, vol. 169, 173-210.
[6] C. C. Jahnke, V. Subramanyan, D. T. Valentine, On the convection in an enclosed container with unstable side wall temperature distributions, International Journal of Heat and Mass Transfer, 1998, vol. 41, No. 15, 2307-2320.
[7] M. Napolitano, L. Quartapelle, Block ADI Methods for Steady Natural Convection in Two Dimensions, Numerical Methods in Heat Transfer, Edited by R. W. Lewis and K. Morgan, Vol. III, John Willey & Sons Ltd., 1985.
[8] L. E. Howle, Control of Rayleigh-Benard convection in a small aspect ratio container, International Journal of Heat and Mass Transfer, 1997, vol. 40, No. 4, 817-822.
[9] J. G. Maveety, Heat transfer in Rayleigh-Benard convection with air in moderate size containers, International Journal of Heat and Mass Transfer, 1997, vol. 41, No. 4-5, 785-796.
[10] J. A. Liggett, Fluid Mechanics, McGraw-Hill, Ins., New York, 1994.
[11] S. V. Patankar, Numerical Heat Transfer and Fluid Flow, Hemisphere, New York, 1980.
[12] B. Franković, K. Lenić, Numerical analysis of free convection in a solar collector with non-uniform boundary condition, Pooceedings of the International congress EuroSun2002, Bologna, 2002.

TOPLINSKI GUBICI SLOBODNOM KONVEKCIJOM U PLOČASTOM SOLARNOM KOLEKTORU

Sažetak: *U radu su numeričkim putem analizirani toplinski gubici uslijed slobodne konvekcije u zatvorenom zračnom prostoru s izotermnim neravnomjernim rubnim uvjetom. Definiran je matematički model temeljen na Oberbeckovom matematičkom modelu graničnog sloja. Model opisuje dvodimenzijski nestacionarni problem prijelaza topline. Numeričkom metodom konačnih volumena izračunata su polja karakterističnih termodinamičkih veličina kao što su vektori brzina, funkcija toka i raspodjela temperatura. Razvijen je računalni program za rješavanje nestacionarnog dvodimenzijskog prijelaza topline. Analiziran je utjecaj Rayleigh-evog broja na pojavu različitih režima strujanja i prijelaza topline za različite kuteve nagiba domene. Utjecaj različitih režima stujanja na prijelaz topline ispitan je preko lokalnih i prosječnih Nusseltovih brojeva. Rezultati istraživanja primjenjeni su na predviđanje toplinskih gubitaka uslijed slobodne konvekcije unutar aproksimiranog modela solarnog kolektora za različite kuteve nagiba.*

Ključne riječi: toplinski gubici uslijed slobodne konvekcije, solarni kolektor, metoda konačnih volumena, toplinski gubici, Rayleigh-ov broj, lokalni i prosječni Nusselt-ov broj